

EFFECTIVE STIFFNESS OF FLANGED REINFORCED CONCRETE STRUCTURAL WALLS: A NUMERICAL APPROACH

Komaravolu Venkata Purneshwar ⁽¹⁾, Nilanjan Samanta ⁽²⁾, Kaustubh Dasgupta ⁽³⁾

⁽¹⁾ MTech student, Department of Civil Engineering, Indian Institute of Technology, Guwahati, India, p.komaravolu@alumni.iitg.ac.in

⁽²⁾ PhD student, Department of Civil Engineering, Indian Institute of Technology, Guwahati, India, nsamanta@iitg.ac.in

⁽³⁾ Associate Professor, Department of Civil Engineering, Adjunct Faculty, Centre for Disaster Management and Research, Indian Institute of Technology, Guwahati, India, kd@iitg.ac.in

Abstract

For high rise buildings, Reinforced Concrete (RC) shear walls have emerged as a preferred structural element due to their significant contributions to global lateral strength, stiffness, and ductility. The lateral stiffness RC structural walls provide to the building system effectively mitigates structural and non-structural damage by limiting excessive deformation. Therefore, accurately estimating the effective stiffness of structural components under design basis earthquake is crucial for determining the design forces on various structural elements and for assessing the global drift of the building system. Under design basis earthquake the concrete cracks over a significant portion of the shear walls and the reinforcement yields in concentrated locations, and thereby there is a reduction of the initial uncracked stiffness. Various international standards and design codes have prescribed effective stiffness of the RC structural wall as a constant reduction factor to the gross moment of inertia of the wall section. Two major limitations of the constant reduction factor prescribed by current design codes are the lack of identification of the key parameters that influence effective stiffness and the inability to consider the geometrical shape of RC structural walls. The present study has tried to address these two major gap areas. In the current study, a flanged RC structural wall from a previous experimental study is selected, and a finite element (FE) modeling is employed to develop the numerical model. Displacement-controlled nonlinear static analyses are conducted. From past studies on rectangular and non-rectangular RC structural walls, the major influencing parameters related to the effective stiffness of the RC structural wall are identified. Based on the determined parameters, a parametric study is conducted, and finally, an empirical equation of the effective stiffness of the L-shaped wall is presented. The accuracy of the empirical equation is assessed by estimating the coefficient of variation (COV) between the predicted effective stiffness and the FE model-derived effective stiffness.

Keywords: *effective stiffness, flanged shear wall, L-shaped structural wall, nonlinear static analysis.*

1. Introduction

Over the past few decades, seismic design standards have had a transition from the force-based approach to the displacement-based approach. This shift necessitates the quantification of the deformation behavior of structures. In the case of reinforced concrete (RC) wall structures, their stiffness characteristics play a pivotal role in determining the fundamental period, deformation, and distribution of internal force responses among walls. The reduction in the gross stiffness of the RC structural wall depends on the level of earthquake hazard (design basis earthquake or maximum considered earthquake) considered in the design of the RC structures. Typically, under the design basis earthquake (DBE) the yielding of the RC structural wall is expected; hence the effective stiffness of an RC structural wall up to the point of yielding is determined using its cross-sectional moment of inertia (MOI), adjusted by a reduction factor to account for the effects of flexural and shear cracking [1]. In general, the stiffness modifier is prescribed in various design codes to take into account for (a) concrete cracking, (b) the effect of axial load, (c) bond-slip of reinforcement, and (d) anchorage extension. In various design standards, the reduction factors vary between 0.35–0.70 [1]. Previous studies [2,3] have examined the reduction factor and proposed various methods to increase the accuracy of stiffness predictions. For RC structural walls, research has primarily concentrated on developing approaches that incorporate additional design parameters and account for shear deformation in the effective stiffness. However,

investigations on non-rectangular RC structural walls [1,4] suggest that the findings applicable to rectangular RC structural walls may not be directly transferable to non-rectangular configurations. A past study [1] proposed effective stiffness values for T-shaped and U-shaped RC structural walls under different loading directions. However, no research has been identified that specifically addresses the effective stiffness of L-shaped RC structural walls, which are commonly used at the corners of building layouts. Therefore, the present study focuses on the nonlinear behavior of L-shaped RC structural walls and ultimately proposes a simplified expression for their effective stiffness.

2. Significance of Present Study

RC structural elements crack immediately after the application of the lateral load which makes the RC structure more flexible than the uncracked condition. Therefore, the uncracked stiffness is modified under the action of the lateral load to get a reasonable structural response (base shear, deformation, etc.). In general, many design codes specify the constant stiffness modifier which has a lack of identification of the salient parameters that contribute to the effective stiffness. Moreover, previous proposals of effective stiffness for rectangular RC structural walls are not applicable to flanged RC structural walls. In the present study empirical expressions of the effective stiffness of the L-shaped RC structural wall are developed which has taken into account both the significant influencing parameters to the effective stiffness as well as the geometrical shape of the RC structural wall.

3. Definition of Effective Stiffness

For RC structural members, effective stiffness can be defined in different ways, though two methods are predominantly used [1]. The first approach estimates the effective stiffness as the secant slope of the lateral force versus lateral displacement curve, evaluated at the point where the applied force reaches 75% of the nominal flexural strength. The second approach defines the effective stiffness as the stiffness of the wall at the onset of yielding, which occurs when either the first longitudinal reinforcing bar yields or the maximum compressive strain in the concrete at the critical section reaches 0.002.

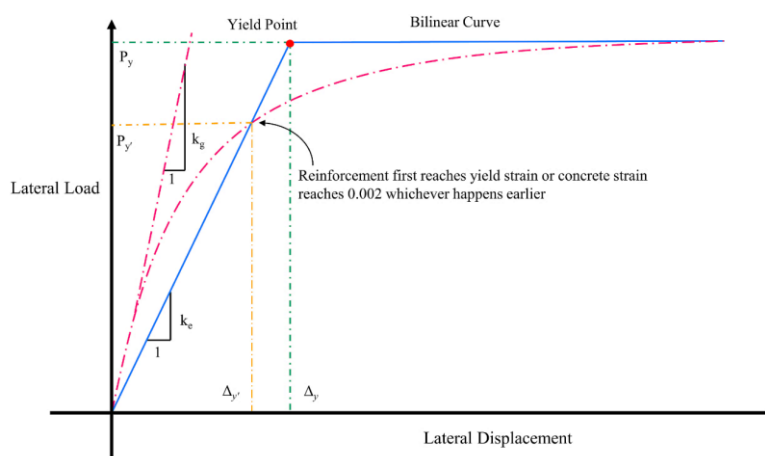


Figure 1. Definition of effective stiffness.

4. Salient Past Studies on Effective Stiffness of Rectangular RC Structural Wall

Based on the parametric study, Fenwick and Bull [2] proposed a relationship between the effective moment of inertia (I_e) and the moment of inertia of an uncracked concrete section (I_g) for cantilever walls which is expressed in Eq. (1) such as:

$$\frac{I_e}{I_g} = 0.267 \left(1 + 4.4 \frac{N}{A_g f'_c} \right) \left(0.62 + \frac{190}{f_y} \right) (0.76 + 0.005 f'_c) \quad (1)$$

Paulay and Priestley [3] proposed Eq. (2) to relate the effective moment of inertia of the wall cross-section at first yield in the extreme fiber (I_e) to the moment of inertia of the uncracked gross concrete section (I_g). The expression was proposed considering the effect of yield strength of longitudinal reinforcement (f_y) and axial load ratio ($P_u/(f_c' A_g)$).

$$I_e = \left(\frac{100}{f_y} + \frac{P_u}{f_c' A_g} \right) I_g \quad (2)$$

Unlike previous researchers, Paulay and Priestley [3] accounted for shear deformation contributions also to the wall stiffness and proposed the following Eq. (3) to evaluate the effective stiffness for structural walls with aspect ratios less than 4.0.

$$I_w = \frac{I_e}{1.2+F}, \text{ where } F = \frac{30I_e}{H^2 t_w l_w} \quad (3)$$

In the above equation, the shear deformation contribution to effective wall stiffness is reflected by wall height (H), wall thickness (t_w), and wall length (l_w).

5. Salient Past Studies on Effective Stiffness of Flanged RC Structural Wall

Numerous studies have been carried out to examine the seismic performance of non-rectangular RC walls. It is worth mentioning here that compared to rectangular RC walls, experimental or numerical investigations regarding flanged or non-rectangular RC walls are limited. A few experimental investigations conducted by Beyer et al. [5], Thomsen and Wallace [4], and Brueggen [6] have helped us to understand the behavior of flanged shear walls. Thomsen and Wallace [4] found that the stiffness of the T-shaped walls is much higher compared to that of the rectangular RC walls of similar height they tested. Brueggen [6] reported that the effective stiffness of the T-shaped wall for web parallel flange-in-tension direction loading was around 30% larger than that of the effective stiffness for flange-in-compression direction loading. Zhang and Li [1] performed a numerical study to find out the effective moment of inertia of flanged RC shear walls and proposed empirical equations for T-shaped RC structural walls for both web parallel flange-in-tension and flange-in-compression. The proposed empirical equations are:

For T-shaped RC structural wall for web parallel flange-in-tension

$$\frac{I_e}{I_g} = 2.35 \frac{P_u}{f_c' A_g} + \frac{185}{f_y} \quad (4)$$

For T-shaped wall for web parallel flange-in-compression

$$\frac{I_e}{I_g} = 1.75 \frac{P_u}{f_c' A_g} + \frac{125}{f_y} \quad (5)$$

6. Formulation of Stiffness Modifier

The in-plane behaviour of RC structural walls is widely considered as single curvature bending. Furthermore, most of the design standards assume cantilever action under the action of lateral load for RC structural wall; therefore, the effective stiffness commonly expressed in the form of stiffness modifier (κ) such as:

$$\kappa = \frac{K_e}{K_g} = \frac{I_e}{I_g} \quad (6)$$

Where K_e is the effective stiffness of the structural member and the K_g is the gross stiffness of the structural member. The effective MOI is related to effective stiffness such as:

$$K_e = \frac{3E_c I_e}{H^3} \quad (7)$$

Where E_c is the concrete modulus elasticity and H is the wall height. Shear deformation in slender RC structural walls has been observed to contribute a significant portion of the total deformation [3]. To

determine the shear deformations of the RC shear wall, the diagonal deformation is measured at the bottom storey of the wall according to Massone and Wallace [7]. The schematic diagram of the shear deformations at the wall base is presented in Fig. 2. Finally, based on Eq. (8) the original shear deformation is estimated.

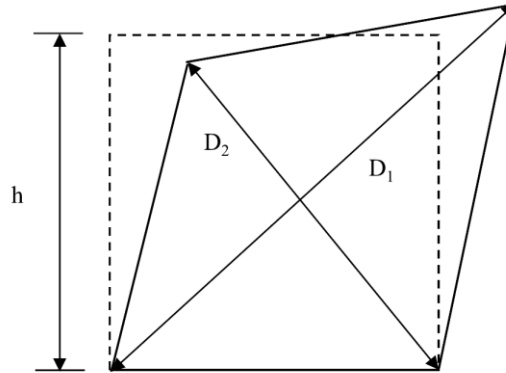


Figure 2. Estimation of shear deformation at the wall base.

$$\Delta_{S_original} = \frac{\sqrt{D_1^2 - h^2} - \sqrt{D_2^2 - h^2}}{2} \quad (8)$$

However, Massone and Wallace [7] have indicated that this method is erroneous if the center of rotation of the bottom storey does not coincide with the geometric center of the storey height; hence the shear deformation is coupled with flexural deformation. In the present study, according to the suggestion of Massone and Wallace [7], the following correction is made in the measurement of shear deformation:

$$\Delta_{S_Corrected} = \Delta_{S_Original} + (0.5 - \alpha\theta h) \quad (9)$$

Where θ is storey level rotation, h is the storey height and α is the relative distance from the top of the first storey to the centroid of the curvature distribution. In the current study, α is taken as 0.67 considering the triangular distribution of curvature [7]. Finally, to get the effective flexural stiffness (K_w), the effective stiffness of the wall (K_e) is reduced by taking into account the influence of the shear deformation such as:

$$K_w = \frac{K_e \Delta_f}{\Delta_f + \Delta_s} = P_f K_e \quad (10)$$

Considering the pure cantilever action, the following expression can be written:

$$I_w = P_f I_e \quad (11)$$

Where Δ_f and Δ_s are the flexural and shear deformation of the wall at first yield, respectively. P_f is the portion of flexure deformation in total deformation for the wall at first yield.

7. Numerical Modelling and Validation

In the current study, the numerical model i.e., a three-dimensional (3D) finite element (FE) model is developed for the parametric analysis in the general-purpose software suite ABAQUS 6.14 which is capable of solving both linear and nonlinear problems. Ni and Lu [8] investigated the seismic behavior of three T-shaped RC walls built with high-strength reinforcement using quasi-static reverse cyclic load. One of the T-shaped wall specimens designated as T-0.1 F in the study of Ni and Lu [8] has been considered in the current study for the verification of the accuracy of the FE model. The details of the crack pattern of the test specimen are also available in previous literature [8]. The aspect ratio (H/l_w) of the test specimen was 2 which qualifies the wall to be slender and exhibit flexural-dominant behavior.

The axial load ratio of the test specimen was 0.1 and the specimen was built with high-strength steel (HRB 600) except for boundary element stirrups (HRB 400). The average characteristic compressive strength of the concrete for the test specimen T-0.1 F was found to be 35 MPa.

The constitutive model of concrete is defined according to the isotropic concrete damage plasticity (CDP) model. The CDP parameters considered in the adopted FE model of the current study are specified in Table 1. According to past studies [9,10], the uniaxial compressive and tensile response of concrete is determined whereas the response of the rebar is taken according to the experimental results. The constitutive model of concrete and steel rebar is presented in Fig. 3.

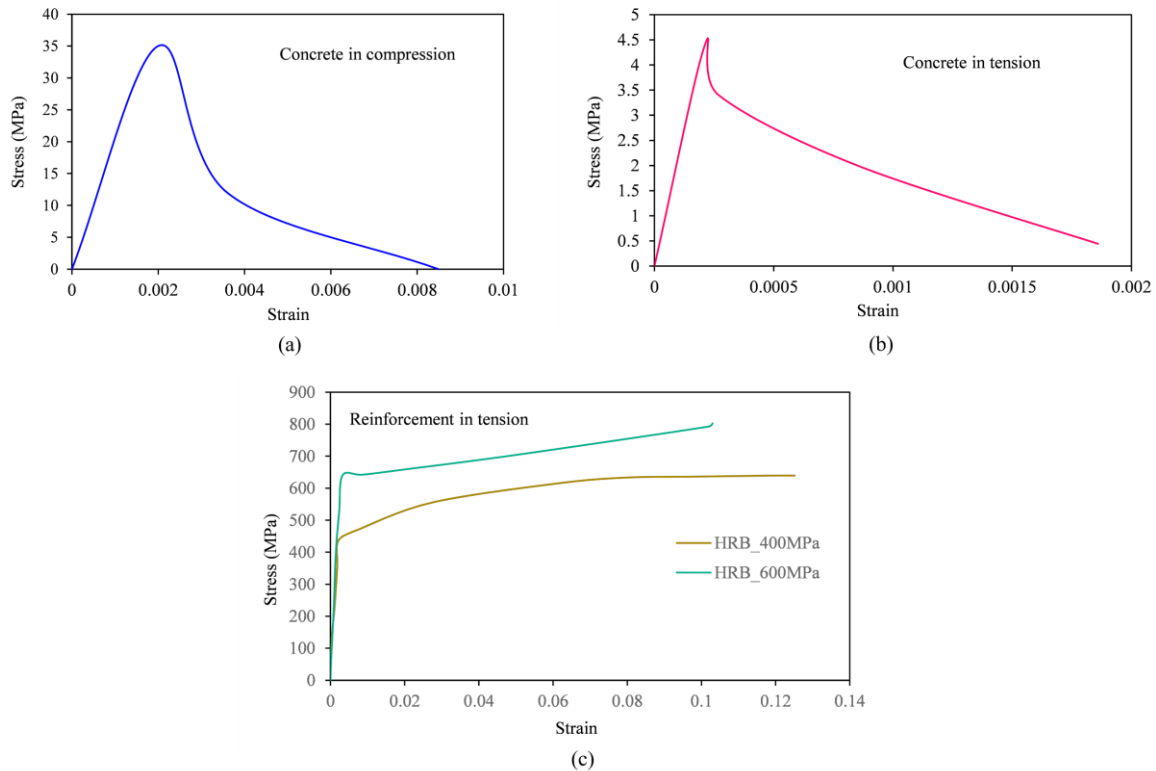


Figure 3. Stress-strain relationship for a) Concrete in uniaxial compression; b) Concrete in uniaxial tension; c) Steel reinforcement.

Concrete elements are modeled as eight-node solid linear brick elements having reduced integration with hourglass control (C3D8R) from ABAQUS/Standard element library. Reinforcement bars are modeled as wire features integrated with the two-node 3D linear truss element (T3D2). Reinforcement bars are considered to be embedded into concrete by using the embedded element constraints which ensures strain compatibility of reinforcement with adjacent concrete. Tie constraints are used in the interface of the loading beam and T-shaped RC wall which ensures no relative motion between them. Similarly, Tie constraints are also used in the interface of the T-shaped RC wall and the pedestal base. All degrees of freedom (DOFs) at the bottom of the pedestal base are considered to be restrained. In the current study, the rotational degrees of freedom (DOF) about the X-axis, the rotational DOF about the Y-axis, and the translational DOF about the Z-axis are made restrained which facilitates the avoidance of the web parallel out-of-plane bending of T-shaped RC wall and rotational movement of T-shaped RC shear walls about the vertical axis of the wall which mimics the actual experimental boundary condition. Fig. 4 shows the typical FE model of the T-shaped RC wall.

Table 1. CDP parameters considered for the material definition of concrete

ψ	e	σ_{b0}/σ_{c0}	K_c	μ
55°	0.1	1.16	0.667	0.01

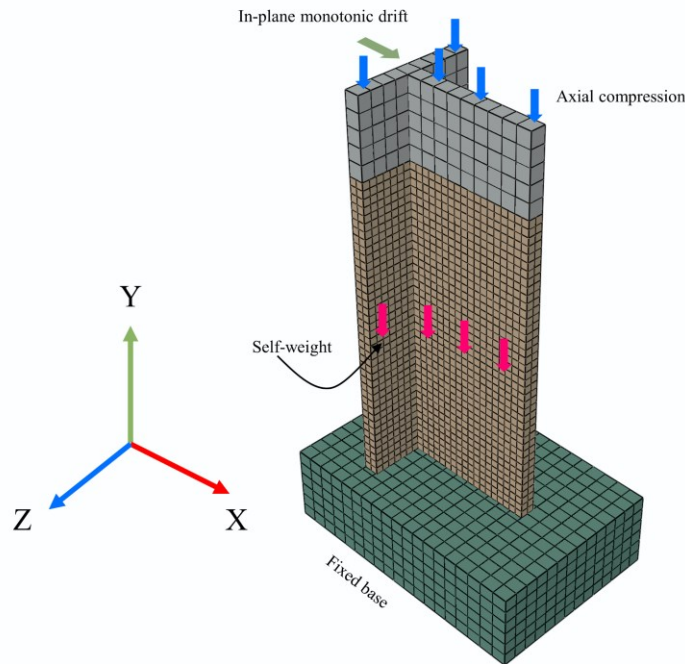


Figure 4. FE model of the T-shaped RC structural wall.

In the current study, the loading is applied in two phases. In the first phase, the self-weight and external axial load is applied and in the second phase, the monotonic load is given in a displacement-controlled manner at the reference point which kinematically couples all nodes of the loading beam. Although analysis involving reverse slow cyclic displacement is the best method to predict the response of the wall, nonetheless the current study adopts monotonic displacement due to time constraints. The monotonic load-drift relationship is compared with the backbone curve of the experimental load-drift relationship of T-0.1 F which is shown in Fig. 5a. Mesh-sensitivity analysis is also accomplished which is shown in Fig. 5b and based on the convergence, the optimum mesh size is decided as 50 mm.

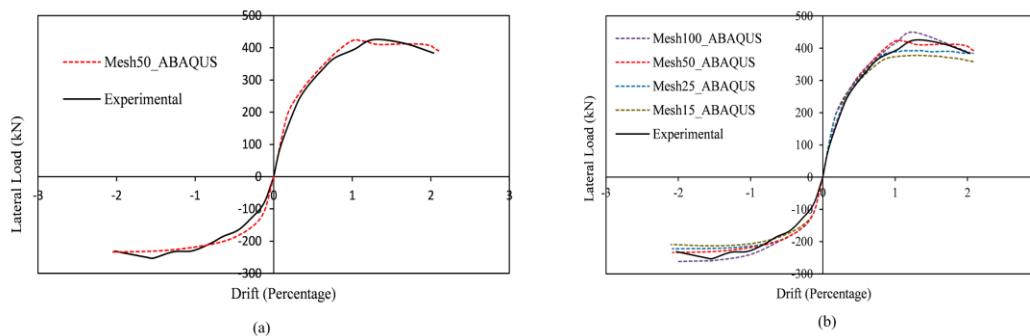


Figure 5. Lateral load-drift relationship for T-0.1 F: a) Numerical result vs. experimental result; b) Mesh sensitivity study

8. Parametric Study for Effective Stiffness

Based on the previous studies [1,3], the following parameters are found to be sensitive for estimating the effective stiffness such as axial load ratio (ALR), aspect ratio (H/l_w) of the wall, yield strength of longitudinal steel rebar (f_y), flange length (b_w). The range of these considered parameters are presented

in Table 2. It is worth mentioning here that unless otherwise specified, the parametric study with zero axial load ratio invariably means that only the self-weight of the structural wall is considered. In this study, the aspect ratio of the numerical L-shaped RC structural wall is taken as 2 which ensures flexure dominant failure mode. All the walls are considered to have characteristic cube compressive strength of 30 MPa. The percentage of longitudinal reinforcement in the web and flange is kept at 0.5% and the spacing between both longitudinal and transverse web rebar is kept at 150mm.

Table 2. Summary of the parameters considered

Aspect ratio	Flange length (b_w) in meter	ALR	Yield strength (MPa)
2,3,4	0.5,1,1.2,1.5,1.7,2.4,3.4,3.6,5.1	0,0.05,0.1,0.2	415,550

9. Results and Discussion

To determine the effective stiffness of L-shaped RC structural walls, the initial load-deformation responses of all the models are recorded. Using these responses, the effective stiffness of each numerical model is calculated based on the previously explained second method. Finally, the effective stiffness is adjusted by applying a reduction factor to account for the influence of shear deformation, as discussed in earlier sections.

9.1. Influence of Axial Load Ratio (ALR)

The influence of axial load ratio on the effective flexural stiffness ratio (K_w/K_g) of L-shaped RC structural walls is presented in Fig. 6a and Fig. 6b for web parallel flange-in-tension and flange-in-compression direction respectively.

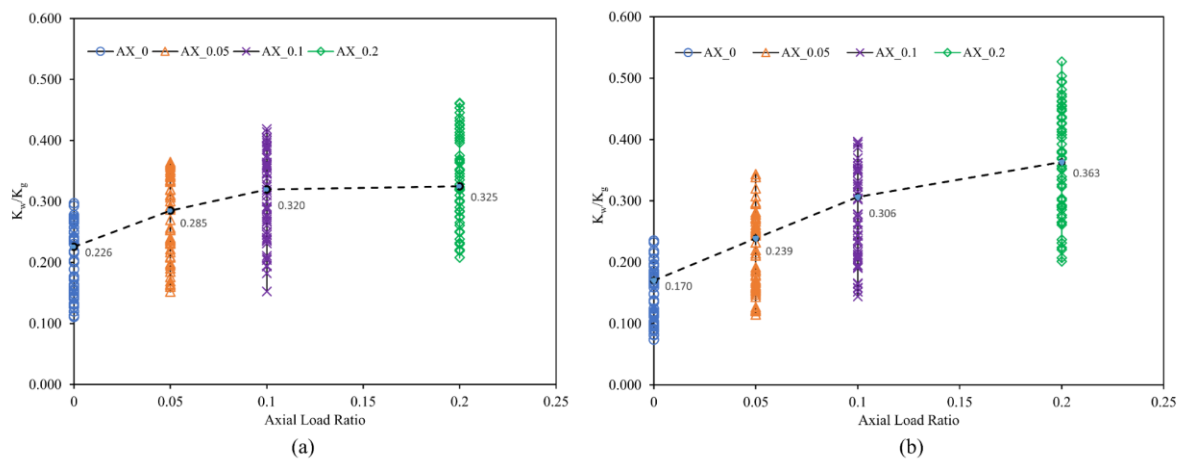


Figure 6. Influence of axial load ratio (ALR) on effective flexural stiffness ratio (K_w/K_g) for (a) Web parallel flange-in-tension; (b) Web parallel flange-in-compression

The results show that as the axial load ratio increases, the effective flexural stiffness ratio also rises. To provide better clarity, the average values corresponding to different axial loads are plotted. For web parallel flange-in-tension loading, an increase in the axial load ratio from 0.0 to 0.2 leads to a 43% rise in the effective flexural stiffness ratio. Although the yield drift increases with higher axial loads, the substantial gain in lateral strength of the RC structural walls ultimately results in an overall increase in the effective flexural stiffness ratio. Despite significant differences in the load-carrying capacity of the wall under web parallel flange-in-tension loading versus flange-in-compression loading, the effective stiffness ratio exhibits less variation. This is attributed to the earlier onset of yielding in the flange-in-compression direction, which leads to a lower yield drift compared to the web-parallel flange-in-tension direction.

9.2. Influence of Aspect Ratio (H/l_w)

The influence of aspect ratio on the effective flexural stiffness ratio (K_w/K_g) of L-shaped RC structural walls is illustrated in Fig. 7a and Fig. 7b for web parallel flange-in-tension and flange-in-compression direction respectively.

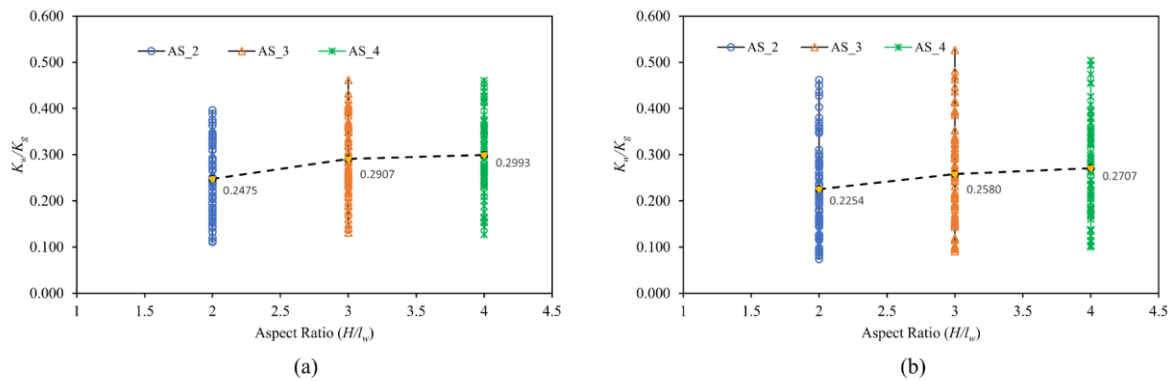


Figure 7. Influence of aspect ratio on effective flexural stiffness ratio (K_w/K_g) for (a) Web parallel flange-in-tension; (b) Web parallel flange-in-compression

From the results, it is quite clear that with an increase in aspect ratio, the effective flexural stiffness ratio (K_w/K_g) increases by 21% for web parallel flange-in-tension direction and by 20% for web parallel flange-in-compression direction. Generally, as the aspect ratio increases, the load-carrying capacity decreases, and the yield drift increases, reducing the effective stiffness ratio K_w/K_g . However, the overall K_w/K_g increases as shear deformation is significant for walls with lower aspect ratios, whereas shear deformation is negligible for walls with higher aspect ratios.

9.3. Influence of Yield Strength (f_y) of Longitudinal Rebar

The influence of the yield strength (FE 415 and FE 550) of vertical rebar on the effective flexural stiffness ratio (K_w/K_g) of L-shaped RC structural walls is shown in Fig. 8a and Fig. 8b for web parallel flange-in-tension and flange-in-compression direction respectively. From the results, it is observed that with an increase in yield strength of vertical rebar, the effective flexural stiffness ratio (K_w/K_g) decreases by about 34% for web parallel flange-in-tension and by about 37% for web parallel flange-in-compression direction. This is expected because with the increase in yield strength of vertical rebar, that load carrying capacity increases marginally but the yield drift increases significantly which finally results large reduction of the effective flexural stiffness ratio.

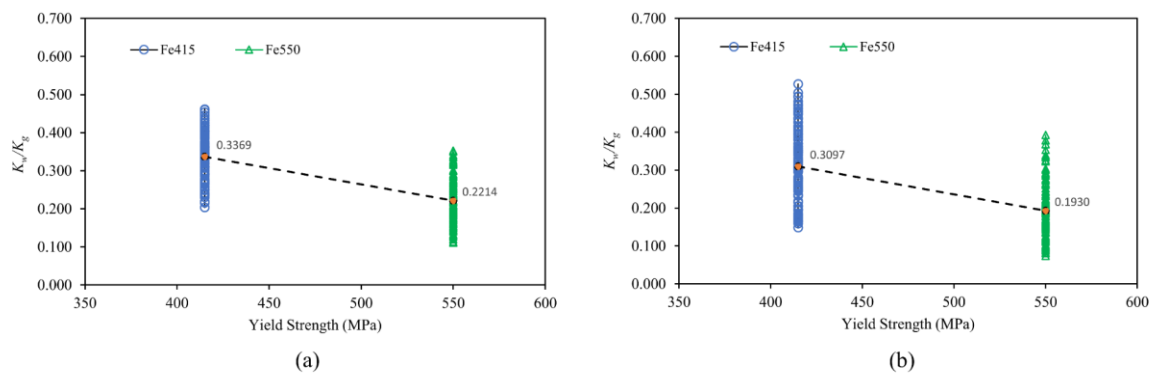


Figure 8. Influence of yield strength (f_y) of longitudinal rebar on effective flexural stiffness ratio (K_w/K_g) for (a) Web parallel flange-in-tension; (b) Web parallel flange-in-compression

9.4. Influence of Flange length (b_w)

In this study, for all numerical models, there are three types of flange lengths such as (a) flange length equals one-third of wall length, (b) flange length equals two-thirds of wall length, and (c) flange length equals wall length. The influence of flange length on the effective flexural stiffness ratio is presented in Fig. 9a and Fig. 9b for web parallel flange-in-tension and flange-in-compression direction respectively.

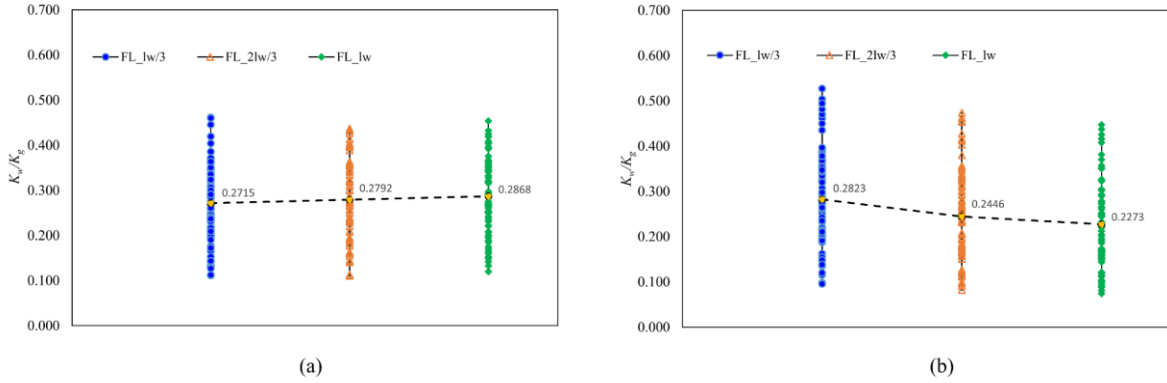


Figure 9. Influence of flange length on effective flexural stiffness ratio (K_w/K_g) for (a) Web parallel flange-in-tension; (b) Web parallel flange-in-compression

For the L-shaped walls web parallel flange-in-tension direction, increasing the flange length from $l_w/3$ (33.3% of the wall length) to l_w (100% of the wall length) does not have a distinct effect on the K_w/K_g ratios. The average value slightly changed from 0.2715 to 0.2868 which indicates a marginal increase in K_w/K_g ratios for any value of flange length in the case of flange-in-tension direction loading. For the web parallel flange-in-compression direction, the average K_w/K_g ratios exhibit a significant decline, dropping from 0.282 to 0.227, corresponding to an approximate 19% reduction. The increase of the flange length increases the gross stiffness (K_g) of the wall section. On the other hand, the K_w of the wall section does not increase proportionally, and the K_w/K_g ratios of the investigated models generally reduce with an increase in the flange length which is evident for the web parallel flange-in-compression direction loading. In the case of web parallel flange-in-tension direction loading, there is a marginal increase of K_w/K_g is observed because the longer flange can be less effective due to the shear lag effect.

9.5. Proposed Empirical Equation of Effective Flexural Stiffness Ratio

Based on the parametric study, the empirical equations for evaluation of the effective stiffness of L-shaped RC structural walls are proposed for different directions of loading with the aid of multiple linear regression following a similar form of equation proposed by Paulay and Priestley [3].

For L-shaped RC structural walls web parallel flange-in-tension direction

$$\frac{K_e}{K_g} = 0.8 \frac{P_u}{f_c' A_g} + \frac{123}{f_y} \quad (12)$$

For L-shaped RC structural walls web parallel flange-in-compression direction

$$\frac{K_e}{K_g} = 1.21 \frac{P_u}{f_c' A_g} + \frac{98}{f_y} \quad (13)$$

Finally, for considering the shear deformation in L-shaped RC structural walls Eq. (13), and Eq. (14) are prescribed. The reduction factors are derived from the empirical relationships of the portions of the flexure deformations with the wall height and the wall length from the FE results.

For L-shaped RC structural walls for web parallel flange-in-tension direction

$$P_f = \frac{1}{1.2 + \frac{22I_e}{H^2 b_w l_w}} \quad (14)$$

For L-shaped RC structural walls for web parallel flange-in-compression direction

$$P_f = \frac{1}{1.2 + \frac{15I_e}{H^2 b_w l_w}} \quad (15)$$

Finally, the effective flexural stiffness ratio of L-shaped RC structural walls is determined as:

$$\frac{K_w}{K_g} = P_f \frac{K_e}{K_g} \quad (16)$$

Finally, the FE model-derived K_w/K_g is compared with the results obtained from the proposed formulae which are shown in Fig. 10. As the figure illustrates, the proposed empirical expression can predict the effective flexural stiffness ratio of these models quite accurately. The mean value and coefficient of variation (COV) for the predicted K_w/K_g ratio over the FE-derived K_w/K_g ratio are 1.12 and 0.199 respectively. The results suggest that the predictions are reasonably consistent and fairly reliable with some scatter.

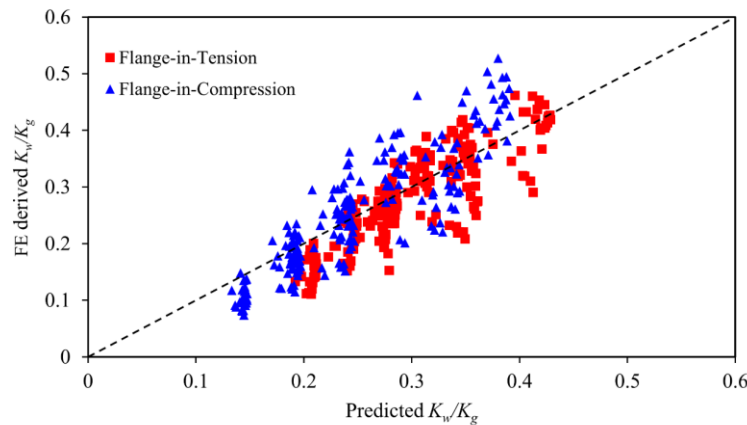


Figure 10. Comparison between Predicted K_w/K_g and FE-derived K_w/K_g

10. Conclusion

The effective flexural stiffness of flanged RC structural walls, as examined in this study, has received limited attention. To address this gap, empirical expressions have been proposed for estimating the effective flexural stiffness of L-shaped RC structural walls frequently used at building layout corners. The major conclusions of the current study can be summarised as:

- The flange in L-shaped RC walls significantly increases the effective stiffness of the wall. The K_w/K_g ratios of L-shaped RC walls are in general higher than those of the rectangular RC walls for the same parameters.
- For the investigated models of L-shaped walls, the average K_w/K_g ratio for the web parallel flange-in-tension direction is higher than that of the flange-in-compression direction.
- An increase in the axial load ratio leads to a rise in the K_w/K_g ratio, while a higher aspect ratio also results in a marginal increase in the K_w/K_g ratio.
- The length of the flange of the L-shaped RC walls reduces the K_w/K_g ratio for web parallel flange-in-compression direction whereas for web parallel flange-in-tension direction the variation of K_w/K_g ratio is insignificant.
- An increase in reinforcement grade of longitudinal reinforcement significantly reduces the K_w/K_g ratio.

- Empirical equations of effective flexural stiffness ratio are proposed by taking into account the shear deformation which will help practical designers to quickly estimate the effective flexural stiffness of L-shaped RC structural walls.

Acknowledgments

The support and resources provided by the Department of Civil Engineering; Indian Institute of Technology, Guwahati are gratefully acknowledged by the authors.

References

- [1] Zhang, Z., Li, B. (2018): Effective Stiffness of Non-Rectangular Reinforced Concrete Structural Walls. *Journal of Earthquake Engineering*, **22**(3), 382–403, doi: <https://doi.org/10.1080/13632469.2016.1224744>
- [2] Fenwick, R. and Bull, D. (2000): What is the stiffness of reinforced concrete walls, *SESOC Journal* **13**(2), 23–32.
- [3] Paulay, T. and Priestley, M. J. N. (1992): *Seismic Design of Concrete and Masonry Structures*, John Wiley and Sons, New York.
- [4] Thomsen, J., Wallace, W (1995): Displacement based design of reinforced concrete structural walls: An experimental investigation of walls with rectangular and T-shaped cross-sections, *Report No. CU/CEE-95-06*, Civil and environmental engineering, Clarkson university
- [5] Beyer, K., Dazio, A., Priestley, M. J. N. (2008): Quasi-static cyclic tests of two U-shaped reinforced concrete walls. *Journal of earthquake engineering*, **12**(7), 1023–1053, doi: <https://doi.org/10.1080/13632460802003272>
- [6] Brueggen (2009): Performance of T-shaped Reinforced Concrete Structural Walls under Multi-Directional Loading, *Dissertation*, University of Minnesota
- [7] Massone, M., Wallace, W (2004): Load-Deformation Responses of Slender Reinforced Concrete Walls, *ACI Structural Journal*, 101-S12, doi: [doi:10.1016/j.engstruct.2017.02.050](https://doi.org/10.1016/j.engstruct.2017.02.050)
- [8] Ni, X., Lu, N. (2022): Cyclic tests on T-shaped concrete walls built with high-strength reinforcement. *Journal of Earthquake Engineering*, **26**(11), 5721–5746, doi: <https://doi.org/10.1080/13632469.2021.1884626>
- [9] Karthik, M. M., Mander, J. B. (2011): Stress-block parameters for unconfined and confined concrete based on a unified stress-strain model. *Journal of Structural Engineering*, **137**(2), 270–273, doi: [https://doi.org/10.1061/\(ASCE\)ST.1943-541X.0000294](https://doi.org/10.1061/(ASCE)ST.1943-541X.0000294)
- [10] Wahalathantri, B., Thambiratnam, D., Chan, T., Fawzia, S. (2011): A material model for flexural crack simulation in reinforced concrete elements using ABAQUS, *In Proceedings of the first international conference on engineering, designing and developing the built environment for sustainable wellbeing* (pp. 260–264), Queensland University of Technology.